

Article

# Multilayer-Forming Behavior of Cr Nitrides and Carbides for Thermoreactive Deposition

Kyeongmo Park <sup>1</sup>, Jun-Ho Kim <sup>2,\*</sup>, Sunkwang Kim <sup>2</sup>  and Namhyun Kang <sup>1,\*</sup> 

<sup>1</sup> Department of Materials Science and Engineering, Pusan National University, Busan 46241, Korea; parkkmo@naver.com

<sup>2</sup> Dongnam regional division, Korea Institute of Industry Technology, Yangsan 50635, Korea; skkim82@kitech.re.kr

\* Correspondence: jhkim81@kitech.re.kr (J.-H.K.); nhkang@pusan.ac.kr (N.K.); Tel.: +82-55-367-9403 (J.-H.K.); +82-51-510-3027 (N.K.)

Received: 4 May 2018; Accepted: 28 May 2018; Published: 30 May 2018



**Abstract:** The effect of a nitride layer on the forming behavior of CrN and (Cr, Fe)<sub>7</sub>C<sub>3</sub> multilayers for thermoreactive deposition (TRD) was investigated. Plasma nitriding followed by TRD (PN-TRD) produced a larger coating thickness than the case of direct TRD with no plasma nitriding. For PN-TRD, an Fe<sub>2-3</sub>N layer of 10 μm in thickness was produced on AISI 52100 steels using plasma nitriding, followed by TRD using a mixed powder composed of 30 wt % Cr, 2 wt % NH<sub>4</sub>Cl, and 68 wt % Al<sub>2</sub>O<sub>3</sub>. During TRD at 800 °C, a CrN layer of 2 μm in thickness was formed along with a thin layer of mixed carbide (Cr<sub>7</sub>C<sub>3</sub>) and nitride (CrN) on top. As the deposition temperature was increased to 950 °C, a new layer of Cr<sub>7</sub>C<sub>3</sub> was formed underneath the outermost layer composed of mixed Cr<sub>7</sub>C<sub>3</sub> and CrN. At 950 °C, a Cr-rich zone indicated a thickness of ~7 μm. As the deposition time increased to 3 h at 950 °C, a new layer of (Cr, Fe)<sub>7</sub>C<sub>3</sub> was produced at the interface between the CrN formed at 800 °C and the base metal. This layer formed because of the abundant resources of Cr and C provided from the TRD powder and base metal, respectively. The multilayer and interface were concretely filled without the formation of voids as the TRD time increased to 6 h at 950 °C. The TRD process on a pre-nitrided layer was successfully applied to produce multilayers of CrN and Cr<sub>7</sub>C<sub>3</sub>.

**Keywords:** nitriding; TRD; pack cementation; multilayer

## 1. Introduction

The materials request continuously higher performance and improved properties [1]. Specifically, many studies have been conducted to improve the wear resistance of materials. Coating technology can improve wear resistance. Deposition techniques, such as physical vapor deposition (PVD) and chemical vapor deposition (CVD), are widely used in academic research. Furthermore, thermoreactive deposition (TRD) and plasma nitriding (PN) are more widely used for mass production to increase wear resistance [2–5]. In addition, studies on surface treatment using multicoating techniques [6–10] and multilayer formation have been conducted to improve bonding strength and wear resistance [11,12].

In PN, nitrogen is diffused into the base material to form a nitrided layer with high hardness; this improves fatigue, corrosion, and wear resistance, and gives excellent thermal stability with less deformation of the base metal. In particular, PN has a shorter processing time, can be done at lower cost, and offers pollution-free operation. Using PN, one can control the phase of nitride compared to normal nitriding [13,14]. In previous studies [6,15], normal nitriding was successfully used to increase the nitrogen content of the substrate surface for multicoating treatment.

Multilayers formed by PVD and CVD have been reported to have superior adhesion and high wear resistance compared to single layer structures [11,12]. That was because a crack starting from the

coating surface was deflected at the interface between the layers. However, PVD has the disadvantages of high cost and low adhesion compared to other coating technologies, such as CVD and TRD. CVD also has many process variables and a complicated device configuration. By contrast, TRD has the advantages of excellent bonding strength, simple equipment, and capability of mass production. TRD coating is performed in a heat treatment furnace at 800–1250 °C using carbonitride-forming powders, such as vanadium, niobium, tantalum, chromium, molybdenum, and tungsten. There are several process techniques incorporating salt baths, fluidized beds, and pack cementation [16]. In the surface treatment based on TRD, factors affecting the growth of the coating layer include temperature, time, powder composition, and base metal. The longer the time, the thicker the coating layer becomes, and the higher the temperature, the more the growth is promoted. The composition of the powder depends on the ratio of the mixed powders and the catalyst used [16–21]. To form a carbide, it is necessary for the base metal to contain at least 0.3 wt % C [18,22], and the carbide thickness becomes thicker as the C content increases [20,23]. Therefore, a multilayer having high hardness formed using TRD is more likely to be applied to the material that requires wear resistance, than that by PVD and CVD.

In this study, we applied PN to increase the nitrogen content of the base material and a Cr-carbonitride multilayer with high hardness, corrosion, and wear resistance was formed on high-carbon steel through TRD coating [24,25]. In the TRD process, the integrity of the coating layer and the diffusion behavior of the coating powder components were investigated with respect to temperature and time, and the formation behavior of multilayers was studied.

## 2. Experimental Details

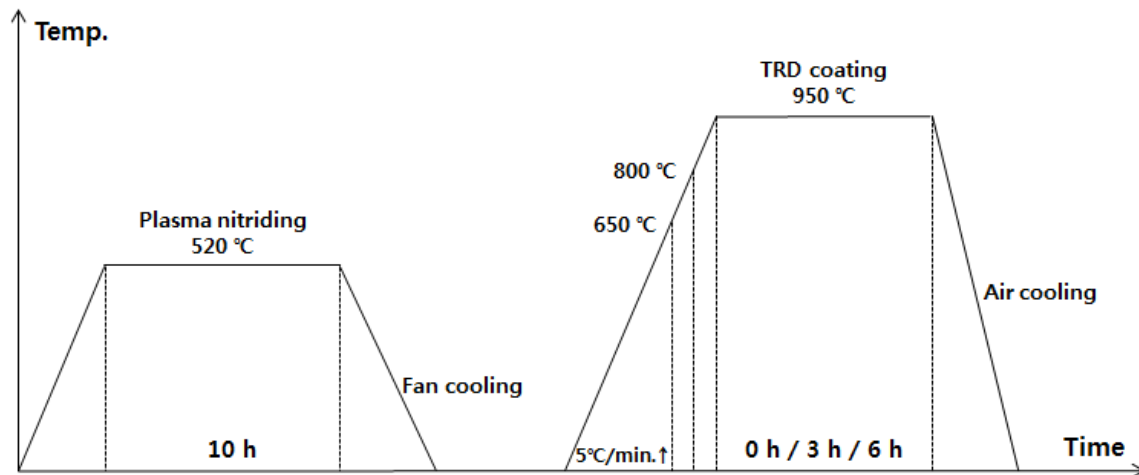
The base material used for the TRD was a high-carbon steel (AISI 52100 steel), with a square pillar of 5 × 5 × 10 mm. The composition of the base material is given in Table 1. Figure 1 shows a schematic diagram of the multicoating treatment. PN (PN40/60, Rübigen, Wels, Austria) was conducted at 520 °C for 10 h. During TRD coating, a heating rate of 5 °C/min was maintained, and specimens were air cooled when they reached 650 °C, 800 °C, and 950 °C. It took 126, 156, and 186 min from the room temperature to reach 650, 800, and 950 °C, respectively. Also, for the study of the TRD layer over time at 950 °C, specimens were kept for 3 and 6 h, followed by air cooling.

All specimens were cleaned with ethanol prior to PN, and then placed in the same place in the furnace for nitriding. The chamber was pumped down to  $3 \times 10^{-1}$  mbar before hydrogen was loaded, and the specimen was cleaned by hydrogen sputtering for 1 h at a pressure of 5 mbar. PN was conducted at 5 mbar using a 90% N<sub>2</sub>–9% H<sub>2</sub>–1% CH<sub>4</sub> mixed gas. After nitriding, the specimens were cooled in the furnace. TRD coating powders were composed of 30 wt % Cr, 2 wt % NH<sub>4</sub>Cl, and 68 wt % Al<sub>2</sub>O<sub>3</sub>, and a 99.9% high-purity powder of Cr was used in the study [19]. TRD coating was performed by using pack cementation. The mixed powder was placed in a cylindrical alumina crucible having a diameter of 36 mm and a height of 45 mm, and the specimen was placed at the center in the longitudinal direction of the crucible.

The cross section of the coating layer was analyzed by field emission scanning electron microscopy (FE-SEM, MIRA3 LMH, TESCAN, Brno, Czech Republic) and the chemical composition by energy dispersive spectroscopy (EDS, APOLLO XP, AMETEK, Berwyn, PA, USA). The surface of the coating layer was analyzed by X-ray diffraction (XRD, Ultima IV, Rigaku, Tokyo, Japan) using a Cu target. Inorganic crystal structure data (ICSD) of the planar distance was used to match the planar distance measured in XRD [26]. Mapping of Fe, Cr, C, and N elements was done by field emission electron probe microanalysis (FE-EPMA, JXA-8530F, JEOL Ltd., Tokyo, Japan) to analyze the formation behavior of the coating layer.

**Table 1.** Chemical composition of AISI 52100 steel.

Element	C	Cr	Mn	Si	P	S	Cu	Ni	Mo	Fe
wt %	0.95	1.39	0.4	0.31	0.08	0.05	0.12	0.08	0.03	Balanced

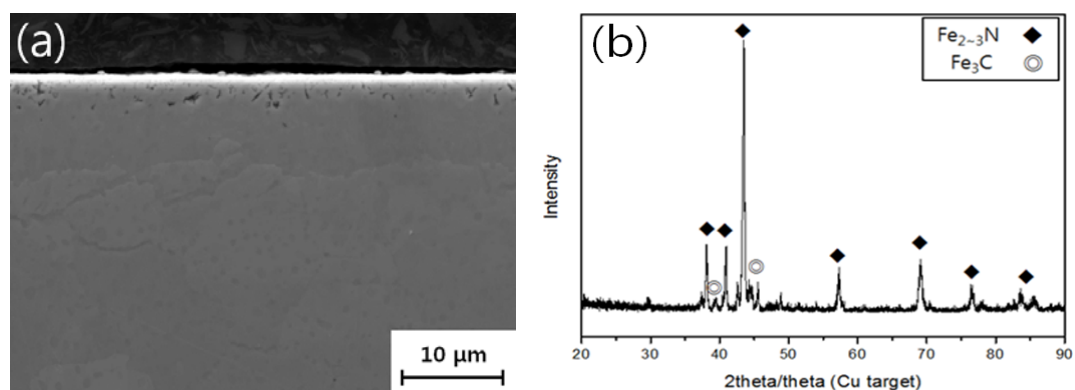
**Figure 1.** Schematic diagram of multicoating treatment, plasma nitriding followed by thermoreactive deposition (PN-TRD).

### 3. Results and Discussion

#### 3.1. Microstructure and Crystal Structure of the Coating Layer

##### 3.1.1. Plasma-Nitrided Layer

Plasma nitriding was preliminarily performed to produce carbonitride by supplying nitrogen with high carbon content of the base material. Figure 2a shows an SEM cross-sectional image of the PN specimen. The nitride was formed to a thickness of  $\sim 10 \mu\text{m}$ , and the typical defect of pores was observed in the outermost surface of the coating layer. Figure 2b shows the XRD pattern measured on the surface of the PN layer.  $\text{Fe}_{2-3}\text{N}$  (ICSD Ref. code: 98-009-3184) was produced on the surface, and it is known to be destabilized and form  $\text{N}_2$  at temperatures  $>450 \text{ }^\circ\text{C}$ . The pores resulting from  $\text{N}_2$  formation are unavoidable on the outermost surface of the coating layer [27]. Furthermore, an  $\text{Fe}_3\text{C}$  (ICSD Ref. code: 98-016-7667) peak was observed because of the  $\text{CH}_4$  gas in the gas mixture used for plasma nitriding.

**Figure 2.** Microstructure of plasma-nitrided specimen: (a) cross-sectional view using SEM; and (b) surface measured using XRD pattern.

### 3.1.2. Thermoreactive Deposited Layer

To obtain a Cr-carbonitride multilayer, a pre-nitrided layer was first formed on the base metal using PN, followed by TRD coating using Cr powder. To investigate the effect of PN before TRD on the forming behavior, TRD-coated specimens (hereinafter, direct-TRD) without a PN layer and TRD-coated PN specimens (hereinafter, PN-TRD) were analyzed. Figure 3a,c compares the cross sections of direct-TRD and PN-TRD specimens, respectively, for 6 h at 950 °C. Direct-TRD produced a coating layer with a thickness of ~10  $\mu\text{m}$ , and a single coating layer was formed. The XRD pattern in Figure 3b shows that the coating layer consisted of  $\text{Cr}_7\text{C}_3$  (ICSD Ref. code: 98-008-7129) and a small amount of CrN (ICSD Ref. code: 98-062-6334). The latter contribution can be explained as follows: because the concentration of  $\text{N}_2$  in the gas atmosphere increased as a result of the decomposition of the  $\text{NH}_4\text{Cl}$  in the mixed powder used in the TRD coating, CrN formed at the outermost surface [19].

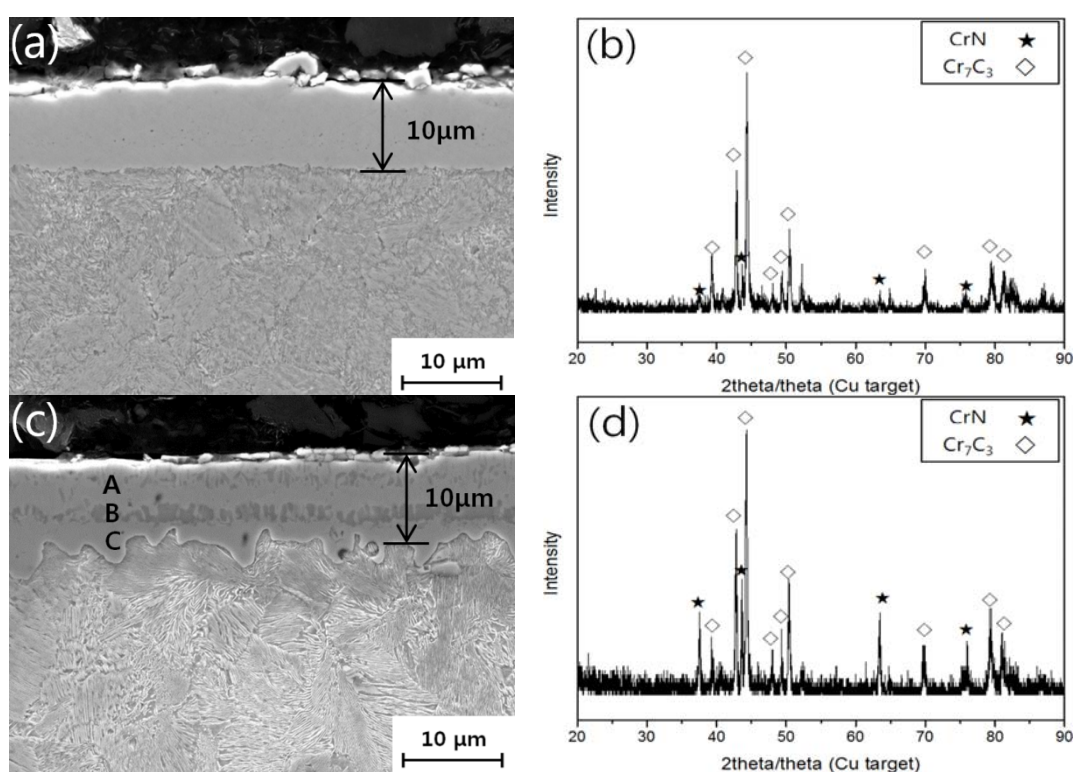


**Figure 3.** Cross-sectional microstructure of direct-TRD specimen (a,b) and PN-TRD (c,d); (a) cross-sectional SEM image; (b) XRD pattern of the direct-TRD coated at 950 °C; (c) cross-sectional SEM image; and (d) XRD pattern of the PN-TRD coated at 950 °C for 6 h.

Figure 3c shows a cross-sectional SEM image of the PN-TRD specimen. The thickness of the coating layer was ~10  $\mu\text{m}$ , and multilayers of dark gray and bright gray were formed. Table 2 gives the EDS analysis measured at points A, B, and C in the multilayer, as indicated in Figure 3c. Carbon contents at points A and C were mostly the same, being ~30 at %. The summation of Fe and Cr contents was ~70 at %. The Cr content at point A was higher than that of point C, and the Fe content was higher at point C than at point A. This is because the Cr diffused into the coating layer from the powder and Fe is supplied from the base material during the TRD reaction. Point B (dark gray) contained a small amount of Fe and C, and most of the material was composed of Cr and N. At point A, there was also a discontinuous microstructure of dark-gray color, which was identified as a CrN layer. The EDS analysis in SEM was reliable for proving the existence of chromium carbides and nitrides, because the base metal was AISI 52100 steel, having C of 0.95 wt %, and TRD after nitriding was conducted in the study. From the XRD results in Figure 3d, higher CrN peaks were found in the

PN-TRD specimens. In addition, no phase related to Fe carbide was observed on the XRD pattern, but it was found that Fe formed a mixed carbide together with Cr through EDS. Compared to the standard  $\text{Cr}_7\text{C}_3$  peak of the XRD database, all peaks of  $(\text{Fe}, \text{Cr})_7\text{C}_3$  are known to have some shifts [21]. As a result of comparing the contents of Fe, Cr, C, and N and XRD patterns through EDS, A and C layers were identified as  $(\text{Fe}, \text{Cr})_7\text{C}_3$ , and the B layer was identified as CrN. Therefore, it was found that the composite coating layer formed through PN-TRD had a multilayer structure of CrN and  $(\text{Fe}, \text{Cr})_7\text{C}_3$ .

**Table 2.** Chemical composition at points A, B, and C indicated in Figure 3c.

Position	Fe (at %)	Cr (at %)	C (at %)	N (at %)
A	26.8	42.7	30.5	-
B	0.6	55.4	5.6	38.4
C	39.7	29.3	31.0	-

### 3.2. Formation Behavior of the Coating Layer with Respect to Temperature

Figure 4 compares the coating behavior of direct-TRD specimens at temperatures of 650 °C, 800 °C, and 950 °C. The direct-TRD specimen showed no change in its surface, even when the process temperature reached 650 °C. When the process temperature was increased to 800 °C, a coating layer gradually formed on the surface portion, and, at 950 °C, a coating layer with a thickness of ~4 μm was formed. Figure 4d lists the chemical composition measured at point A indicated in Figure 4c. Nitrogen was not observed, and it was judged that  $(\text{Cr}, \text{Fe})_7\text{C}_3$  was formed because the total content of Fe and Cr was ~66.1 at %, and the content of C was ~33.9 at % C.

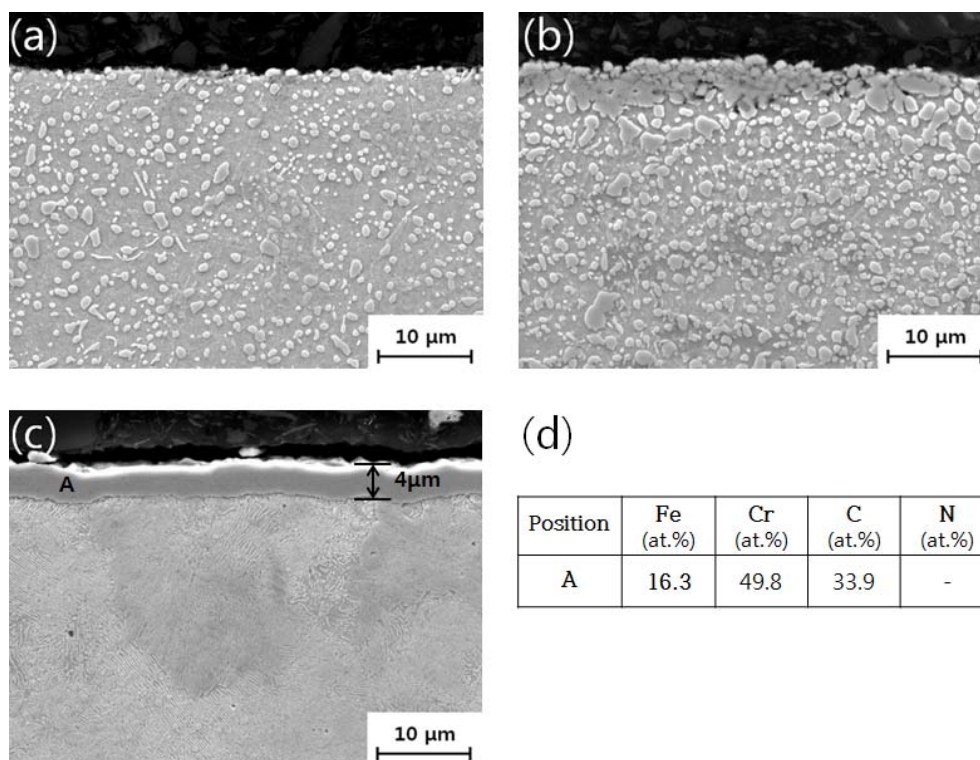


**Figure 4.** Formation behavior of direct-TRD layer with respect to temperature: (a) 650 °C; (b) 800 °C; (c) 950 °C; and (d) chemical composition at point A indicated in Figure 4c.

Figure 5 shows the behavior of coating layer formation of PN-TRD specimens at 650 °C, 800 °C, and 950 °C. The PN-TRD specimen was in the middle of the decomposition of  $\text{Fe}_2\text{N}_3$  when it reached

650 °C. Approaching 800 °C, a coating layer of ~3 µm in thickness was formed. When the temperature reached 950 °C, a composite layer of ~7 µm in thickness was formed, and the layer was divided into A (bright gray) and B (dark gray) layers, as indicated in Figure 5c. The composition of A and B layers is given in Figure 5d. The content of Fe and Cr in the A layer is ~69.2 at %, and the content of C is ~30.8 at %. Therefore, it is considered to be (Cr, Fe)<sub>7</sub>C<sub>3</sub>. The B layer was CrN, with Cr and N content of ~ 91.3 at %.

The PN-TRD specimen formed a coating layer of 3 µm at 800 °C, which thickened to 7 µm at 950 °C. The multilayer thickness of the PN-TRD specimen was 3 µm thicker than the 4 µm thickness of the direct-TRD specimen at 950 °C. The PN-TRD specimen decomposed Fe<sub>2-3</sub>N nitride to provide a high nitrogen concentration on the surface, and reacted with the Cr powder before the diffusion of N, thereby producing a CrN layer rapidly at 800 °C. As the TRD progressed to 950 °C, both C and Cr diffused from the base material and TRD powder, respectively, reacting to form (Cr, Fe)<sub>7</sub>C<sub>3</sub> on the CrN coating layer. In addition, compared to the direct-TRD process, the PN-TRD process exhibited porosity, as indicated with red arrows in Figure 5a–c, and a high coating speed. This can probably be attributed to the pores formed by the decomposition of the nitride serving as a diffusion path for Cr, thereby accelerating the formation of the coating layer [27–29]. Given the thickness of the composite layer, the optimum temperature of the TRD process is determined to be 950 °C.

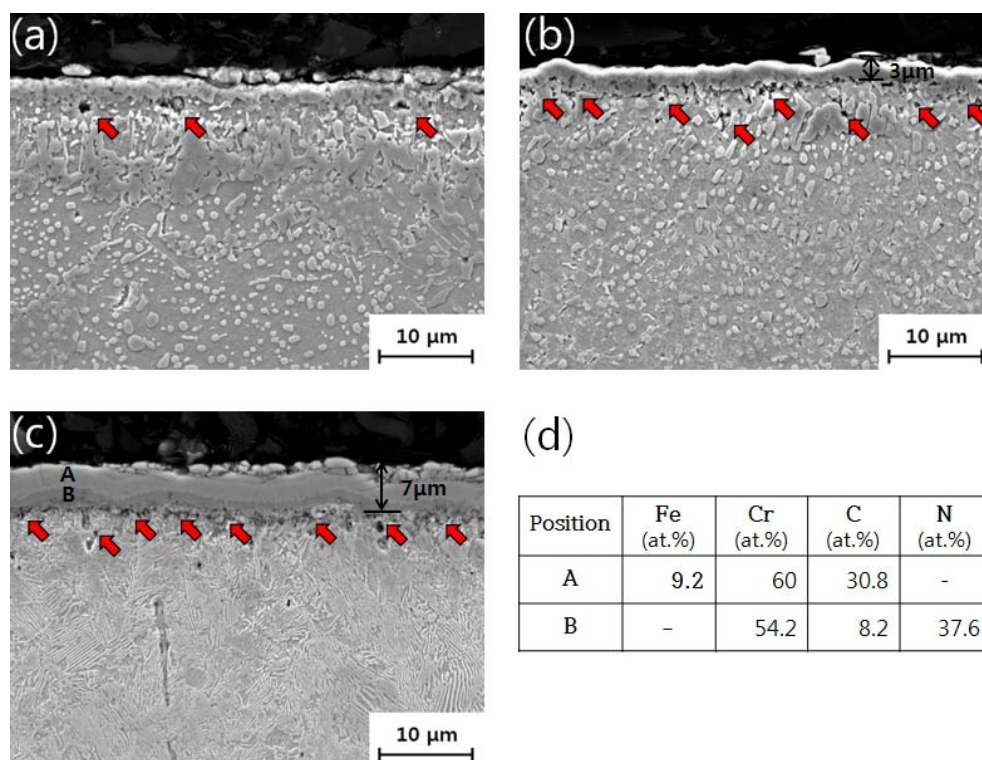


**Figure 5.** Formation behavior of PN-TRD layer with respect to temperature: (a) 650 °C; (b) 800 °C; (c) 950 °C; and (d) chemical composition at points A and B indicated in (c).

### 3.3. Formation Behavior of Coating Layers with Respect to the TRD Time at 950 °C

Figure 6 compares the formation stages of the direct-TRD and PN-TRD coating layers at the optimum TRD temperature (950 °C) with respect to the retention time (0–6 h). The direct-TRD specimen had a layer thickness of 4 µm at 0 h and 9 µm at 3 h. After 6 h at 950 °C, the thickness of the coating layer increased from 9 µm to 10 µm. Although the growth rate of the coating layer decreased, the interface between the coating layer and the base material became uniform.

The PN-TRD coating layer exhibited thicknesses of  $\sim 7 \mu\text{m}$  at 0 h,  $\sim 9 \mu\text{m}$  at 3 h, and  $\sim 10 \mu\text{m}$  at 6 h. The PN-TRD coating produced the following multilayers: a CrN layer with a dark gray color and a  $\text{Cr}_7\text{C}_3$  layer with a bright gray color. The CrN layer retained the same thickness of  $\sim 2 \mu\text{m}$  as time increased to 6 h. These results indicate that the N resource is entirely consumed to form CrN, as the temperature increased to  $950 \text{ }^\circ\text{C}$ . However, when the specimen was maintained at  $950 \text{ }^\circ\text{C}$  for 3 h, a  $(\text{Cr, Fe})_7\text{C}_3$  layer was formed under the CrN layer, and the number of pores decreased (as indicated by the red arrows in Figure 6e). As the process time increased to 6 h,  $(\text{Cr, Fe})_7\text{C}_3$  was further grown under the CrN layer, and the porosity continued to decrease. Comparing direct-TRD (Figure 6c) and PN-TRD (Figure 6f) images at 6 h, one sees that the boundary between the direct-TRD layer and the base material was uniform but that the PN-TRD coating layer had an irregular boundary. Under the CrN layer (Figure 6e), the  $\text{Cr}_7\text{C}_3$  layer with porosity indicated a larger thickness than that with no porosity. Therefore, it can be seen that the porosities assist the diffusion of Cr derived from the TRD coating powder.

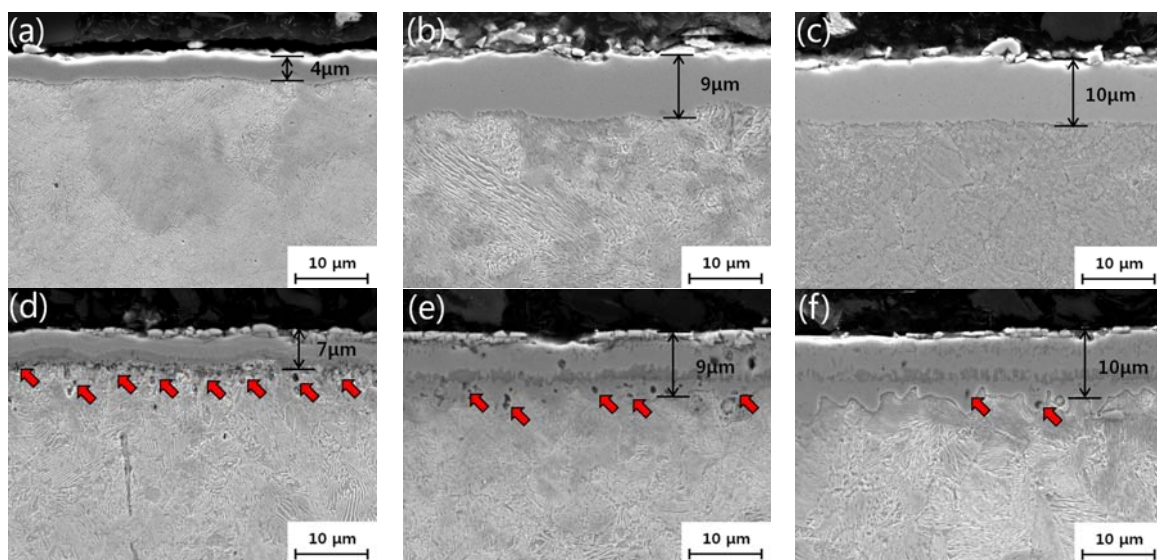


**Figure 6.** Formation behavior of direct-TRD and PN-TRD layers at  $950 \text{ }^\circ\text{C}$  with respect to time: (a–c) direct-TRD for 0, 3, and 6 h, respectively; (d–f) PN-TRD for 0, 3, and 6 h, respectively.

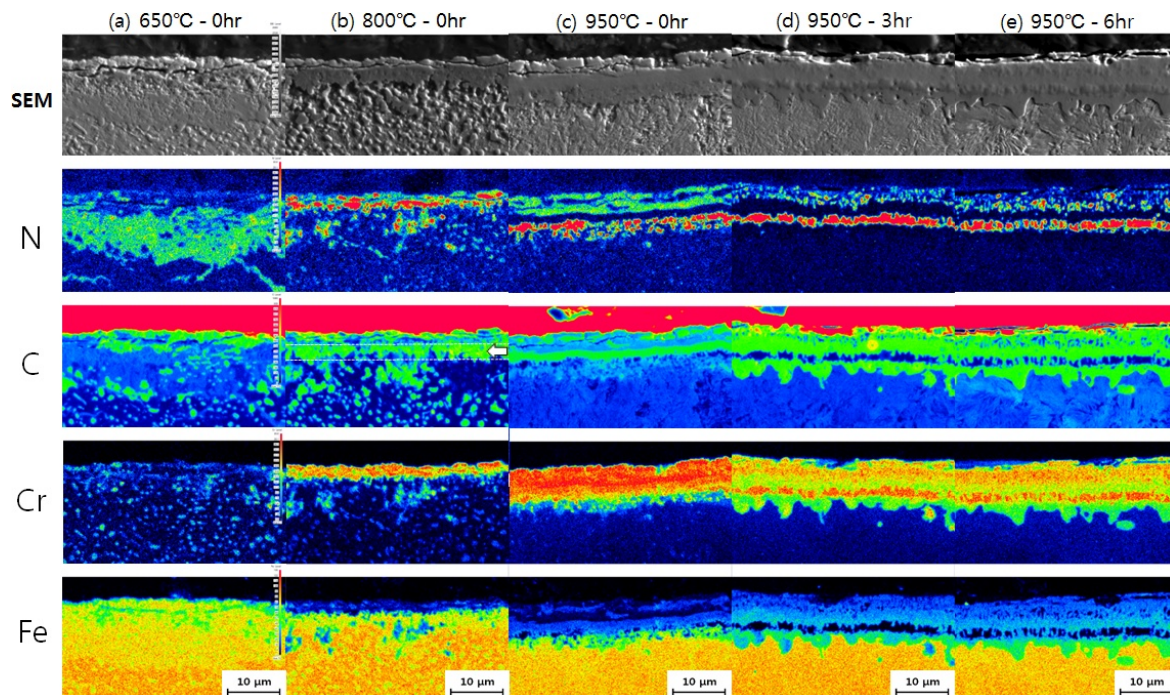
### 3.4. Diffusion of Fe, Cr, C, and N During the Formation of Coating Layers

Figure 7 compares the extent to which the diffusion of Fe, Cr, C, and N elements contributes to the formation of the PN-TRD composite layer with respect to the TRD temperature and time. The color scale bar is represented in Figure 7a. The blue- and red-color area represent, respectively, the lowest and highest content of alloying elements. For  $650 \text{ }^\circ\text{C}$ , N was widely spread under the surface, and the decomposition of the nitride was incomplete (Figure 7a).

At  $800 \text{ }^\circ\text{C}$ , both Cr and N distributions were concentrated on the surface, and the distribution thickness of N decreased compared to that at  $650 \text{ }^\circ\text{C}$  (Figure 7b). Comparing the distribution of N and Fe, one sees that there is a deficiency of Fe in the region where N is abundant. Therefore, it is considered that the  $\text{Fe}_{2.3}\text{N}$  nitride completely decomposed and reacted with Cr to form CrN. C was diffused to the outermost surface on the CrN layer, and a  $\text{Cr}_7\text{C}_3$  layer was partly produced on the CrN layer. Furthermore, a carbon-rich layer (indicated by the white arrow) was present under the CrN coating layer. The nitrogen supplied from the decomposition of  $\text{Fe}_{2.3}\text{N}$  and the carbon supplied from the base material diffused to the surface and reacted with the carbonitride-forming element, Cr, to form a composite layer of carbide and nitride. When low-carbon steels were coated with Cr powder, a decarburized layer was formed under the Cr carbide layer [30]. However, the high-carbon steels

used in this study showed a C-rich zone without a decarburized zone, and C diffused to the surface, thereby producing a small amount of Cr carbides in the outermost layer.

As the TRD temperature increased to 950 °C, Cr was present on the surface at a thickness of ~7 μm, as shown in Figure 7c. In addition, N exists intensively at the interface between the base material and the coating layer, thereby producing a CrN layer with a thickness of 2–3 μm. A C-rich zone existed above the CrN layer with a thickness of 1–2 μm, and, on the outermost surface, abundant N and C were observed with a thickness of 2–3 μm. That is, the Cr-rich layer having a thickness of 7 μm was composed of a composite layer of (CrN + Cr<sub>7</sub>C<sub>3</sub>)–Cr<sub>7</sub>C<sub>3</sub>–CrN. From the cross-sectional SEM image (Figure 6d), it can be seen that this is consistent with the composite layer having a thickness of ~7 μm. The C-rich zone under the CrN layer, which was found in Figure 7b, diffused above the CrN layer as the TRD process temperature increased to 950 °C, and reacted with incoming Cr to form Cr<sub>7</sub>C<sub>3</sub> on the CrN layer. Approaching 950 °C, the N distribution region was divided into two distinct layers. The N distribution in the outermost layer was probably formed by the formation of CrN resulting from the increased concentration of N<sub>2</sub> in the gas atmosphere from the decomposition of NH<sub>4</sub>Cl in the TRD coating mixed powder. This was also observed in direct-TRD specimens, as can be seen from the XRD results in Figure 3a.



**Figure 7.** Diffusion mapping of Fe, Cr, C, and N during coating layer formation with TRD temperature and time using EPMA.

Figure 7d shows the component behavior of a PN-TRD specimen maintained at 950 °C for 3 h. Compared with the results of the specimen at 950 °C for 0 h, the diffusion of N was insignificant, and the distribution thickness of C and Cr increased to 9–12 μm. N was concentrated in the interface between the base material and the coating layer, as was the case for the CrN layer, indicated in Figure 7c, and the thickness of the CrN layer remained the same, with no variation, even when the TRD process lasted for 3 h at 950 °C. Furthermore, a layer containing Cr was observed in the outermost layer composed of a composite layer of CrN + Cr<sub>7</sub>C<sub>3</sub>. The whole composite layer enriched with Cr consisted of (CrN + Cr<sub>7</sub>C<sub>3</sub>)–Cr<sub>7</sub>C<sub>3</sub>–CrN, as in the case of the 950 °C 0 h specimen. However, unlike the 0 h specimen, the 950 °C 3 h specimen produced a new layer enriched with Cr, C, and Fe under the CrN layer formed at the interface between the base material and the coating layer. This layer is estimated to

be  $(\text{Cr, Fe})_7\text{C}_3$ . This phenomenon became more evident in the 950 °C 6 h specimen, as indicated in Figure 7e. In the  $(\text{Cr, Fe})_7\text{C}_3$  layer, the concentration of Cr decreased and that of Fe increased as the base material was approached.

Figure 8 summarizes the behavior of composite layer formation with temperature and time in the PN-TRD process. When the PN-TRD specimen was held at 950 °C for 6 h, a CrN coating layer was formed on the interface between the base material and the coating layer, and a  $\text{Cr}_7\text{C}_3$  layer and a mixed  $(\text{Cr}_7\text{C}_3 + \text{CrN})$  layer were formed closer to the surface. Below the CrN layer at the interface,  $(\text{Cr, Fe})_7\text{C}_3$  was produced. The total thickness of the composite layer was 10–12 μm. The composite layer was in the order of  $(\text{CrN} + \text{Cr}_7\text{C}_3)\text{--Cr}_7\text{C}_3\text{--CrN--}(\text{Cr, Fe})_7\text{C}_3$  from the outermost layer.

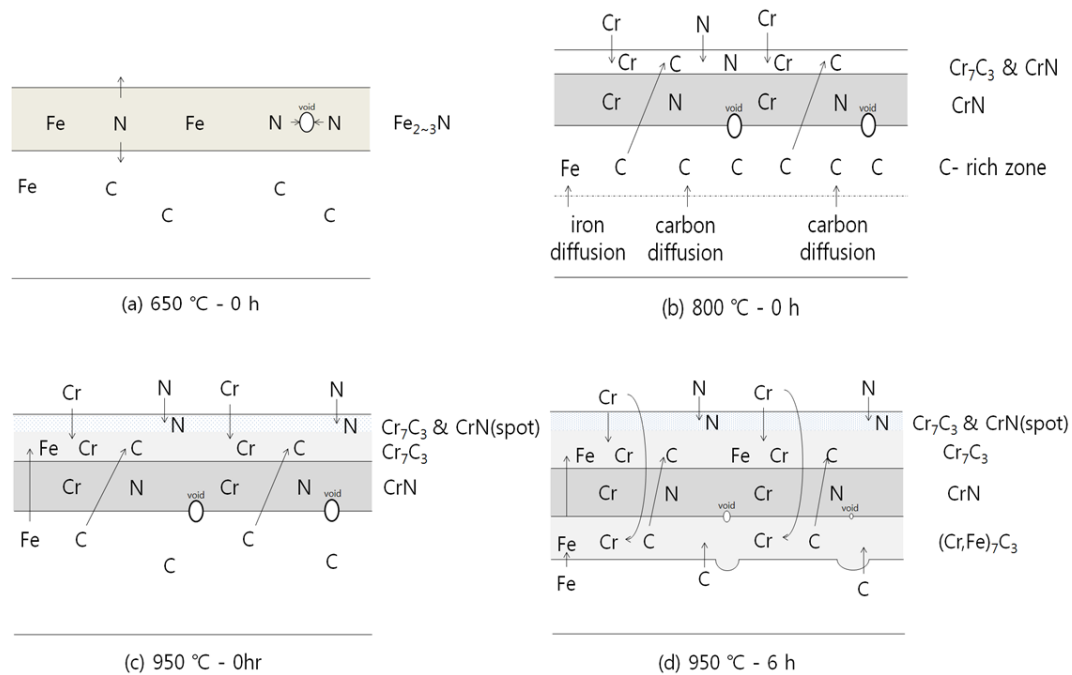


**Figure 8.** Schematics of multilayer formation for PN-TRD specimens as a function of TRD temperature and time: (a) 650 °C for 0 h; (b) 800 °C for 0 h; (c) 950 °C for 0 h; and (d) 950 °C for 6 h.

#### 4. Conclusions

In this study, an  $\text{Fe}_{2-3}\text{N}$  layer was formed by plasma nitriding on AISI 52100 steel, followed by TRD coating using Cr powder to form a composite coating layer. The influence of Fe, Cr, C, and N diffusion on the formation of the composite layer was studied as a function of the TRD temperature and time.

- (1) In the direct-TRD process, a coating layer of ~4 μm thickness was formed at 950 °C. Mostly, a  $\text{Cr}_7\text{C}_3$  layer was formed and a small amount of CrN phase formed.
- (2) The PN-TRD process showed a faster coating layer formation rate than the direct-TRD process, and a coating layer of ~7 μm thickness was formed at 950 °C. When the TRD temperature was increased to 800 °C, the rich N supplied from the decomposition of  $\text{Fe}_{2-3}\text{N}$  and the Cr supplied from the TRD powder reacted to produce the CrN layer with a thickness of 2 μm. The outermost surface layer consisted of a mixed  $(\text{Cr}_7\text{C}_3 + \text{CrN})$  layer. Furthermore, a C-rich zone was formed under the CrN layer.
- (3) When the TRD temperature was increased to 950 °C, a 2 μm-thick  $\text{Cr}_7\text{C}_3$  layer was formed between the  $(\text{Cr}_7\text{C}_3 + \text{CrN})$  layer, and the CrN layer formed at the interface between the base material and the coating layer. The whole composite layer consisted of  $(\text{Cr}_7\text{C}_3 + \text{CrN})\text{--Cr}_7\text{C}_3\text{--CrN}$  and had a thickness of ~7 μm.

- (4) For the 950 °C 6 h specimen, the coating layer had the same elemental distribution as that of the 3 h specimen and the thickness of 10–12 µm. However, the multilayer and interface were concretely filled without the formation of voids as the TRD time increased to 6 h at 950 °C. The TRD process on the pre-nitrided layer was successfully applied to produce a multilayer of  $(\text{CrN} + \text{Cr}_7\text{C}_3)\text{-Cr}_7\text{C}_3\text{-CrN-(Cr, Fe)}_7\text{C}_3$  from the outermost layer.

**Author Contributions:** K.P., J.K. and N.K. conceived and designed the experiments; K.P. and S.K. performed the experiments; K.P., J.K. and N.K. analyzed and discussed the data; K.P. and N.K. wrote the paper.

**Acknowledgments:** This work was supported by the Future Material Discovery Project of the National Research Foundation of Korea (NRF) funded by the Ministry of Science, ICT and Future Planning (MSIP) of Korea (NRF-2016M3D1A1023534) and a National Research Foundation of Korea (NRF) grant funded by the Korean government (MSIT) through GCRC-SOP (Grant no. 2011-0030013).

**Conflicts of Interest:** The authors declare no conflict of interest.

## References

- Oil and Colour Chemists' Association, Raw Materials and Their Usage. In *Surface Coatings*; Springer: Dordrecht, The Netherlands, 2012; Volume 1, ISBN 9789401045346.
- Warcholinski, B.; Gilewicz, A. Tribological properties of CrN<sub>x</sub> coatings. *J. Achiev. Mater. Manuf. Eng.* **2009**, *37*, 498–504.
- Maury, F.; Douard, A.; Delclos, S.; Samelor, D.; Tendero, C. Multilayer chromium based coatings grown by atmospheric pressure direct liquid. *Surf. Coat. Technol.* **2009**, *204*, 983–987. [[CrossRef](#)]
- Aghaie-Khafri, M.; Fazlalipour, F. Vanadium carbide coatings on die steel deposited by the thermo-reactive diffusion technique. *J. Phys. Chem. Sol.* **2008**, *69*, 2465–2470. [[CrossRef](#)]
- Binder, C.; Bendo, T.; Hammes, G.; Klein, A.N.; de Mello, J.D.B. Effect of Nature of Nitride Phases on Sliding Wear of Plasma Nitrided Sintered Iron. *Wear* **2015**, *332–333*, 995–1005. [[CrossRef](#)]
- Hakami, F.; Sohi, M.H.; Ghani, J.R.; Ebrahimi, M. Chromizing of plasma nitrided AISI 1045 steel. *Thin Solid Films* **2011**, *519*, 6783–6786. [[CrossRef](#)]
- Hakami, F.; Sohi, M.H.; Ghani, J.R. Duplex surface treatment of AISI 1045 steel via plasma nitriding of chromized layer. *Thin Solid Films* **2011**, *519*, 6792–6796. [[CrossRef](#)]
- Taktak, S.; Ulker, S.; Gunes, I. High temperature wear and friction properties of duplex surface treated bearing steels. *Surf. Coat. Technol.* **2008**, *202*, 3367–3377. [[CrossRef](#)]
- Wei, C.Y.; Chen, F.S. Characterization on multi-layer fabricated by TRD and plasma nitriding. *Mater. Chem. Phys.* **2005**, *90*, 178–184. [[CrossRef](#)]
- Cao, H.L.; Luo, C.P.; Liu, J.W.; Zou, G.F. Phase transformations in low-temperature chromized 0.45wt% C plain carbon steel. *Surf. Coat. Technol.* **2007**, *201*, 7970–7977. [[CrossRef](#)]
- Gilewicz, A.; Warcholinski, B. Tribological properties of CrCN/CrN multilayer coatings. *Tribol. Int.* **2014**, *80*, 34–40. [[CrossRef](#)]
- Warcholinski, B.; Gilewicz, A. The properties of multilayer CrCN/CrN coatings dependent on their architecture Plasma Process. *Plasma Process. Polym.* **2011**, *8*, 333–339. [[CrossRef](#)]
- Hirsch, T.; Clarke, T.G.R.; da Silva Rocha, A. An in-situ study of plasma nitriding. *Surf. Coat. Technol.* **2007**, *201*, 6380. [[CrossRef](#)]
- Clarke, T.G.R.; da Silva Rocha, A.; Reguly, A.; Hirsch, T. In situ XRD measurements during plasma nitriding of a medium carbon steel. *Surf. Coat. Technol.* **2005**, *194*, 283. [[CrossRef](#)]
- Lee, K.; Kang, N.; Bae, J.; Lee, C.W. Microstructural behavior of nitriding compound layer for Nb-carbonitride coating grown by thermo-reactive diffusion process. *Met. Mater. Int.* **2016**, *22*, 842–848. [[CrossRef](#)]
- Arai, T. *Thermo-Reactive Deposition/Diffusion Process ASM Handbook: Heat Treating*; ASM International: Materials Park, OH, USA, 1991; Volume 4.
- Ozdemira, O.; Sen, S.; Sen, U. Formation of chromium nitride layers on AISI 1010 steel by nitro-chromizing treatment. *Vacuum* **2007**, *81*, 567–870. [[CrossRef](#)]
- Aghaie-Khafri, M.; Fazlalipour, F.; Phys, J. Kinetics of V(N,C) coating produced by a duplex surface treatment. *Chem. Solids* **2008**, *69*, 2465. [[CrossRef](#)]

19. Wei, C.Y.; Chen, F.S. Thermoreactive deposition coating of chromium carbide by contact free method. *Mater. Chem. Phys.* **2005**, *91*, 192–199. [[CrossRef](#)]
20. Chen, F.S.; Lee, P.Y.; Yeh, M.C. Thermal reactive deposition coating of chromium carbide on die steel in a fluidized bed furnace. *Mater. Chem. Phys.* **1998**, *53*, 19–27. [[CrossRef](#)]
21. Lu, X.J.; Xiang, Z.D. Formation of chromium nitride coatings on carbon steels by pack cementation process. *Surf. Coat. Technol.* **2017**, *309*, 994–1000. [[CrossRef](#)]
22. King, P.C.; Reynoldson, R.W.; Brownrigg, A.; Long, J.M. Cr(N,C) diffusion coating formation on pre-nitrocarburised H13 tool steel. *Surf. Coat. Technol.* **2004**, *179*, 18–26. [[CrossRef](#)]
23. Lee, J.W.; Duh, J.G. Evaluation of microstructures and mechanical properties of chromized steels with different carbon contents. *Surf. Coat. Technol.* **2004**, *177–178*, 525. [[CrossRef](#)]
24. Taktak, S.; Gunes, I.; Ulker, S.; Yalcin, Y. Effect of N<sub>2</sub>+H<sub>2</sub> gas mixtures in plasma nitriding on tribological properties of duplex surface treated steels. *Mater. Charact.* **2008**, *59*, 1784. [[CrossRef](#)]
25. Ghahfarokhi, H.H.; Saatchi, A.; Monirvaghefi, S.M. Corrosion investigation of chromium nitride and chromium carbide coatings for PEM fuel cell bipolar plates in simulated cathode condition. *Fuel Cells* **2016**, *16*, 356. [[CrossRef](#)]
26. Cullity, B.D.; Stock, S.R. *Elements of X-ray Diffraction*, 3rd ed.; Prentice-Hall: New York, NY, USA, 2001; ISBN 9780201610918.
27. Dossett, J.; Totten, G.E. Fundamentals of nitriding and nitrocarburizing. In *ASM Handbook: Steel Heat Treating Fundamentals and Processes*; ASM International: Materials Park, OH, USA, 2013; p. 619. ISBN 9781627080118.
28. Cao, H.L.; Luo, C.P.; Liu, J.W.; Wu, C.L.; Zou, G.F. Formation of a nanostructured CrN layer on nitrided tool steel by low temperature chromizing. *Scr. Mater.* **2008**, *58*, 786. [[CrossRef](#)]
29. King, P.C.; Reynoldson, R.W.; Brownrigg, A.; Long, J.L. Fluidized bed CrN coating formation on prenitrocarburized plain carbon steel. *J. Mater. Eng. Perform.* **2004**, *13*, 431. [[CrossRef](#)]
30. Baggio-Scheid, V.H.; de Vasconcelos, G.; Oliveira, M.A.S.; Ferreira, B.C. Duplex surface treatment of chromium pack diffusion and plasma nitriding of mild steel. *Surf. Coat. Technol.* **2003**, *163–164*, 313–317. [[CrossRef](#)]



© 2018 by the authors. Licensee MDPI, Basel, Switzerland. This article is an open access article distributed under the terms and conditions of the Creative Commons Attribution (CC BY) license (<http://creativecommons.org/licenses/by/4.0/>).